

# Temperature-dependent tunneling electroresistance in Pt/BaTiO<sub>3</sub>/SrRuO<sub>3</sub> ferroelectric tunnel junctions

Wen, Zheng; You, Lu; Wang, Junling; Li, Aidong; Wu, Di

2013

Wen, Z., You, L., Wang, J., Li, A., & Wu, D. (2013). Temperature-dependent tunneling electroresistance in Pt/BaTiO<sub>3</sub>/SrRuO<sub>3</sub> ferroelectric tunnel junctions. *Applied physics letters*, 103(13), 132913-.

<https://hdl.handle.net/10356/101042>

<https://doi.org/10.1063/1.4823580>

---

© 2013 AIP Publishing LLC. This paper was published in *Applied Physics Letters* and is made available as an electronic reprint (preprint) with permission of AIP Publishing LLC. The paper can be found at the following official DOI: <http://dx.doi.org/10.1063/1.4823580>. One print or electronic copy may be made for personal use only. Systematic or multiple reproduction, distribution to multiple locations via electronic or other means, duplication of any material in this paper for a fee or for commercial purposes, or modification of the content of the paper is prohibited and is subject to penalties under law.

*Downloaded on 20 Mar 2024 20:00:00 SGT*

## Temperature-dependent tunneling electroresistance in Pt/BaTiO<sub>3</sub>/SrRuO<sub>3</sub> ferroelectric tunnel junctions

Zheng Wen, Lu You, Junling Wang, Aidong Li, and Di Wu

Citation: *Applied Physics Letters* **103**, 132913 (2013); doi: 10.1063/1.4823580

View online: <http://dx.doi.org/10.1063/1.4823580>

View Table of Contents: <http://scitation.aip.org/content/aip/journal/apl/103/13?ver=pdfcov>

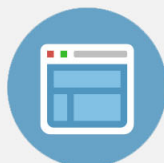
Published by the AIP Publishing

---



## Re-register for Table of Content Alerts

Create a profile.



Sign up today!



# Temperature-dependent tunneling electroresistance in Pt/BaTiO<sub>3</sub>/SrRuO<sub>3</sub> ferroelectric tunnel junctions

Zheng Wen,<sup>1,2,a)</sup> Lu You,<sup>3</sup> Junling Wang,<sup>3</sup> Aidong Li,<sup>1</sup> and Di Wu<sup>1,a)</sup>

<sup>1</sup>National Laboratory of Solid State Microstructures, Nanjing University, Nanjing 210093,

China and Department of Materials Science and Engineering, College of Engineering and Applied Sciences, Nanjing University, Nanjing 210093, China

<sup>2</sup>College of Physics Science, Qingdao University, Qingdao 266071, China

<sup>3</sup>School of Materials Science and Engineering, Nanyang Technological University, Singapore 639798, Singapore

(Received 31 July 2013; accepted 14 September 2013; published online 27 September 2013)

Tunneling electroresistance of Pt/BaTiO<sub>3</sub>/SrRuO<sub>3</sub> ferroelectric tunnel junctions is investigated as a function of temperature. Two distinct resistance states that are dependent on polarization direction in the BaTiO<sub>3</sub> barrier layer and bipolar resistance switching are observed at various temperatures from 10 to 290 K. The ON/OFF current ratio of Pt/BaTiO<sub>3</sub>/SrRuO<sub>3</sub> tunnel junctions increases monotonically with decreasing temperature above 50 K and saturates below 50 K. The enhanced tunneling electroresistance at low temperatures can be ascribed to the suppression of thermally assisted indirect tunneling, which is less sensitive to the polarization reversal of BaTiO<sub>3</sub> compared to the direct tunneling. © 2013 AIP Publishing LLC. [<http://dx.doi.org/10.1063/1.4823580>]

Significant technological advances have recently been achieved in the epitaxial growth of perovskite oxide thin films. Ferroelectricity is observed to exist even in films of only a few nanometers in thickness.<sup>1</sup> This result makes it possible to realize ferroelectric tunnel junctions (FTJs), which are prototype nonvolatile memory elements composed of two metal electrodes separated by an ultrathin ferroelectric layer.<sup>2,3</sup> The ultrathin ferroelectric layer serves as a potential barrier and allows direct quantum mechanical tunneling. The barrier height seen by the tunneling electrons can be electrically modulated via polarization reversal in the ferroelectric barrier. This phenomenon gives rise to electrical switching of the tunneling resistance between low (ON) and high (OFF) levels, i.e., tunneling electroresistance.

The ON/OFF ratio of FTJs varies over a few orders of magnitude as the polarization value, the thickness of ferroelectric barriers, and the screening length of electrodes are changed, in agreement with predictions by Zhuravlev and co-workers.<sup>4</sup> In experiment, a direct correlation between polarization reversal and tunneling electroresistance has been demonstrated by means of scanning probe microscopy, employing conductive-tips as top electrodes, in several nanometer-thick BaTiO<sub>3</sub> (BTO) and PbTiO<sub>3</sub> layers grown on metallic perovskite oxides, such as (La,Sr)MnO<sub>3</sub> (LSMO) and SrRuO<sub>3</sub> (SRO).<sup>5–7</sup> Repetitive switching between two distinct resistance values and good data retention for up to 10 yr have been achieved in FTJs at room temperature using BTO, Pb(Zr,Ti)O<sub>3</sub>, and BiFeO<sub>3</sub> as barriers.<sup>8–13</sup> These results reveal the significant potential utility of FTJs in nonvolatile memory applications with the advantages of non-destructive resistive readout, simple device architecture, and high density data storage.

However, it is well known that defects are present in ferroelectric thin films, and these increase the leakage currents

and may result in significant degradation in overall performance of ferroelectric random access memories and ferroelectric field effect transistors.<sup>14</sup> These defects may also exist in ultrathin ferroelectrics and, as a result, deteriorate resistance switching properties of FTJs. In this work, we report temperature-dependent tunneling electroresistance of Pt/BTO/SRO FTJs from 10 to 290 K. An increased ON/OFF current ratio is observed with decreasing temperature. This result is ascribed to the suppression of phonon-assisted indirect tunneling through localized defects present in the ferroelectric barriers.

Epitaxial BTO/SRO bilayers were deposited on (001) plane of single crystal pseudocubic DyScO<sub>3</sub> substrates by pulsed laser deposition using a KrF excimer laser ( $\lambda = 248$  nm, Coherent COMPexPro205), monitored *in situ* by reflection high energy electron diffraction (RHEED, STAIB Instrumente GmbH). The DyScO<sub>3</sub> substrates were etched by NH<sub>4</sub>F

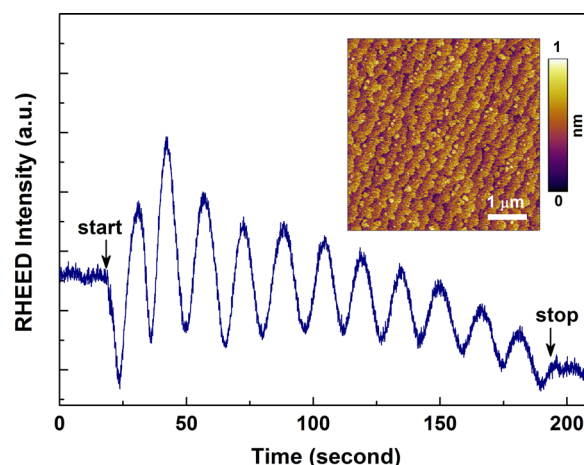


FIG. 1. *In situ* RHEED intensity oscillations during epitaxial growth of BTO on SRO buffered DyScO<sub>3</sub> substrates. The inset shows the typical surface morphology of the BTO/SRO bilayer as measured with atomic force microscopy.

<sup>a)</sup>Authors to whom correspondence should be addressed. Electronic addresses: [zwen@qdu.edu.cn](mailto:zwen@qdu.edu.cn) and [diwu@nju.edu.cn](mailto:diwu@nju.edu.cn).

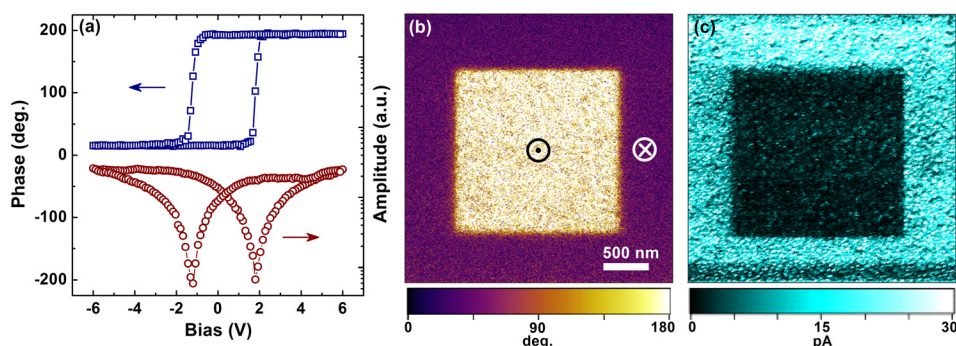


FIG. 2. (a) Local PFM hysteresis loops for the ultrathin BTO film (top: phase signals; bottom: amplitude signals). (b) Out-of-plane phase image and (c) tunneling current mapping over the same area shown in (b).

buffered-HF solution and then annealed at  $1050^{\circ}\text{C}$  for 2 h in flowing  $\text{O}_2$  to form a single-termination step-terrace surface. 12-nm thick SRO electrodes were deposited with  $2.5\text{ J/cm}^2$  laser energy density at 4 Hz repetition, keeping the substrate temperature at  $700^{\circ}\text{C}$  and the  $\text{O}_2$  pressure at 0.05 mbar. BTO layers were deposited with  $1.5\text{ J/cm}^2$  laser energy density and 2 Hz repetition rate at  $750^{\circ}\text{C}$  and 0.005 mbar  $\text{O}_2$  pressure. The thickness of the BTO barrier layer was set at 12 unit-cells (u.c.) by counting the number of RHEED intensity oscillations, as shown in Fig. 1. Clear oscillations of the RHEED intensity reveal layer-by-layer growth of the BTO layer. This growth mode maintains the step-terrace morphology of the substrate with a step height of 0.4 nm, the height of one unit-cell (see inset of Fig. 1). Piezoresponse force microscopy (PFM) and tunneling current mapping of BTO thin films were performed using an Asylum Research Cypher scanning probe microscope with conductive diamond-coated silicon cantilevers (CDT-NCHR, Nano World). Pt top electrodes  $30\text{ }\mu\text{m}$  in diameter were sputter-deposited through a shadow mask. A Keithley 2400 SourceMeter was used to measure resistance switching properties. Temperature-dependent current-voltage (I-V) characteristics of the Pt/BTO/SRO tunnel junctions were measured in a LakeShore CRX-4K probe station by BeCu probes on the electrodes.

As shown in Fig. 2(a), clear hysteresis seen in the PFM loops indicates the ferroelectric nature of the 12-u.c. BTO film at room temperature. The coercive voltages are  $+1.8$  and  $-1.2\text{ V}$ , respectively, as indicated by the minima of the amplitude hysteresis loop. Domains were then written on the BTO layer. BTO was first polarized downward by scanning the conductive-tip biased at  $+4.0\text{ V}$  over an area of  $3.0 \times 3.0\text{ }\mu\text{m}^2$ . Then the central  $1.8 \times 1.8\text{ }\mu\text{m}^2$  area was switched upward by scanning the conductive-tip biased at  $-4.0\text{ V}$ . Fig. 2(b) shows the out-of-plane PFM phase image. The nearly  $180^{\circ}$  phase contrast indicates that the polarizations are antiparallel in the two domains. Subsequently, a tunneling current mapping was performed by scanning a  $+0.5\text{ V}$  biased tip over the two domains shown in Fig. 2(b). As expected, a clear current contrast with respect to the polarization direction of BTO is observed, as shown in Fig. 2(c). The down domain (the ON state) shows a larger tunneling current than that of the up domain (the OFF state), as also seen in the polarization-dependent tunneling resistance of ultrathin BTO and  $\text{PbTiO}_3$  grown on  $\text{SrTiO}_3$  substrates.<sup>6,7</sup>

Pt top electrodes were deposited on BTO layers to produce FTJs. Fig. 3 shows resistance switching properties of the Pt/BTO/SRO tunnel junctions under bipolar pulse cycling. The write pulse of  $+3.0$  and  $-2.0\text{ V}$  were applied

alternately on the Pt electrode to switch the polarization of BTO barrier. After each write pulse, the tunneling resistance was read by a  $+0.1\text{ V}$  pulse. As shown, a repetitive bipolar resistance switching is achieved at room temperature with an ON/OFF ratio of  $\sim 10$ .

The direct tunneling conductance of Pt/BTO/SRO fluctuates below 1% over the temperature region of 10–290 K according to the Stratton temperature correction factor  $\frac{CT}{\sin CT}$ , where  $C \propto 10^{-5}d/\sqrt{\Phi}$  with the barrier width ( $d$ ) in nanometers and the barrier height ( $\Phi$ ) in eV. (Here, the barrier heights are taken from the fits shown in Figs. 4(e) and 4(f).)<sup>15–19</sup> Since the direct tunneling process is almost temperature independent, the I-V characteristics of Pt/BTO/SRO tunnel junctions are measured as a function of temperature to separate the possible contribution from thermally activated conduction. As shown in Figs. 4(a) and 4(b), the currents of the ON and the OFF states decrease with decreasing temperature. Correspondingly, the ON/OFF current ratio, shown in Fig. 4(c), increases with decreasing temperature from 290 to 50 K and saturates below 50 K. The significant temperature dependence of tunneling electroresistance in the Pt/BTO/SRO tunnel junction implies thermally activated contributions in parallel with direct tunneling. A similar phenomenon has also been observed in  $\text{LSMO}/(\text{La,Ca})\text{MnO}_3/\text{BTO}/\text{LSMO}$  FTJs, where the conductance increases significantly with increasing temperature, accompanied with a smearing of the tunneling electroresistance.<sup>12</sup> Yin *et al.* pointed out that, in addition to the direct tunneling, thermally activated indirect tunneling also occurs in  $\text{LSMO}/(\text{La,Ca})\text{MnO}_3/\text{BTO}/\text{LSMO}$  FTJs.<sup>12</sup> This kind of tunneling originates from electron hopping through chains of localized states inside the barrier

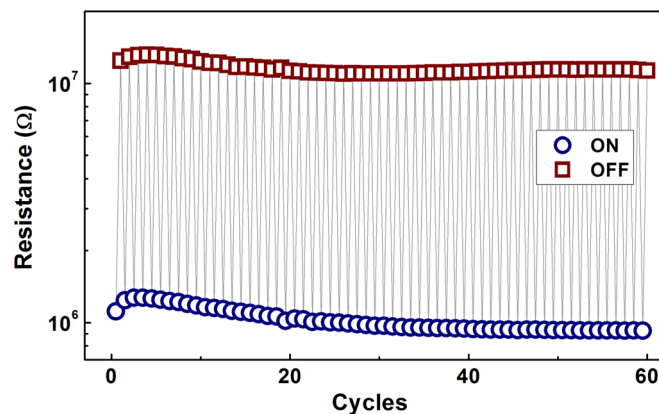


FIG. 3. Resistance switching of Pt/BTO/SRO junctions between the ON and OFF states.



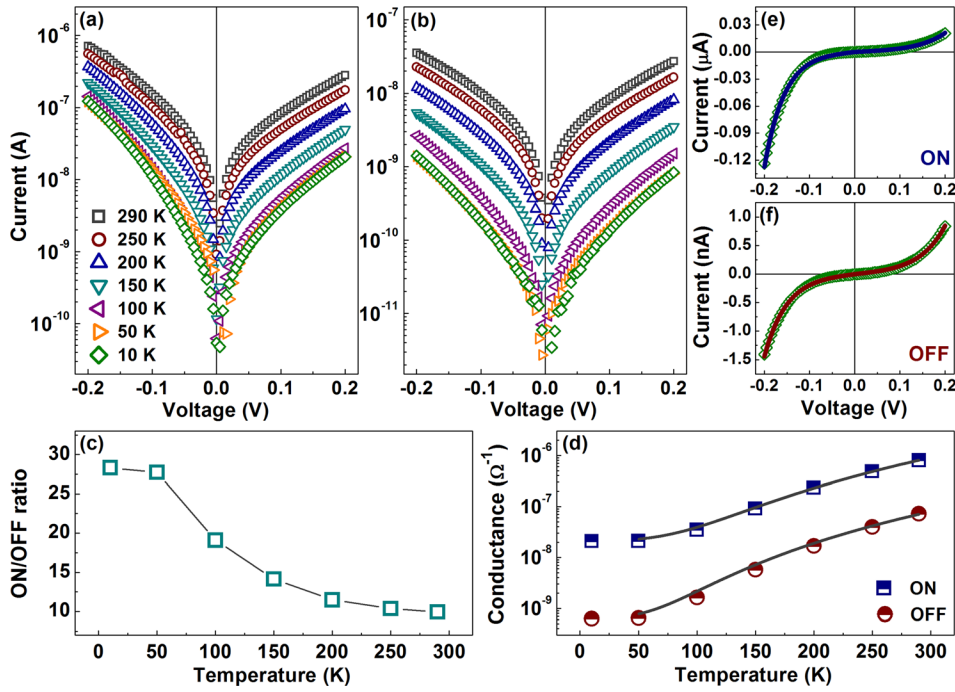


FIG. 4. Temperature-dependent tunneling electroresistance of the Pt/BTO/SRO FTJ, where write pulses of +3.0 and -2.0 V are applied to set the junction to the ON and the OFF states, respectively. Semi-log I-V curves of the ON (a) and the OFF (b) states measured at various temperatures. (c) ON/OFF current ratio at +0.1 V as a function of temperature. (d) Conductance at zero bias as a function of temperature. The solid lines are fits to the GM model. ON (e) and OFF (f) I-V curves at 10 K, where the solid lines are fits to the direct tunneling model.

layer and is associated with the emission (or absorption) of phonons.<sup>18–21</sup> This phonon-assisted indirect tunneling is strongly temperature dependent and less sensitive to polarization reversal, in contrast to the direct tunneling. This tunneling mode has also been frequently observed in magnetic tunnel junctions<sup>18,19,21,22</sup> and can be described by the Glazman-Matveev (GM) model.<sup>18,21–23</sup> The temperature-dependent conductance ( $G$ ) of a tunnel junction through  $N \geq 1$  localized states is given by

$$G = G_{DT} + \sum_{N=1}^{\infty} a_N T^{(N-\frac{2}{N+1})},$$

where  $G_{DT}$  represents the direct tunneling term and  $a_N \propto \exp[-2d/(N+1)\alpha]$  are constants dependent on the radius of the localized states ( $\alpha$ ) and the barrier width ( $d$ ). Note that the expression for  $G(T)$  is applicable for  $eV \ll k_B T$  and is valid when both  $eV$  and  $k_B T$  are smaller than the barrier height.<sup>18,21</sup> With the barrier height close to 1 eV in Pt/BTO/SRO, this expression can be used over the entire temperature range of 10–290 K when the voltage  $V$  is close to 0. As shown in Fig. 4(d), the conductance of the ON and the OFF states at zero bias, i.e.,  $\frac{dI}{dV}|_{V \rightarrow 0}$ , decreases by over about two orders of magnitude with decreasing temperature. The temperature-dependent conductance data from 290 to 50 K can be well fitted using the GM expression with  $N=4$ . Owing to the gradual suppression of the less polarization-sensitive phonon-assisted indirect tunneling, the ON/OFF ratio of Pt/BTO/SRO increases monotonically from 290 to 50 K. As the temperature is further decreased, the ON and the OFF conductance changes little. Correspondingly, the ON/OFF ratio saturates. These results imply that direct tunneling may be predominant in electron transport of Pt/BTO/SRO junctions below 50 K, since the indirect tunneling is substantially suppressed. The I-V curves at 50 and 10 K are almost identical and can be well fitted using the formula for direct tunneling proposed by Gruverman *et al.* based on a

trapezoidal shape potential barrier,<sup>6</sup> as shown in Figs. 4(e) and 4(f). The barrier heights at the Pt/BTO and BTO/SRO interfaces are 0.89 and 0.62 eV, respectively, for the ON state. After polarization switching, the barrier heights change to 1.13 and 0.51 eV, respectively, for the OFF state. The modulation of barrier height is 0.065 eV due to polarization reversal, which yields an ON/OFF ratio of  $\sim 30$  below 50 K, 3 times larger than that at room temperature. The barrier profiles and their polarization dependences in Pt/BTO/SRO tunnel junctions agree well with the previous results reported in the literature.<sup>6,8,10</sup>

In summary, the tunneling electroresistance of Pt/BTO/SRO FTJs has been investigated as a function of temperature. The existence of two distinct resistance states upon polarization reversal is clearly observed. Typical bipolar resistance switching with an ON/OFF ratio of  $\sim 10$  is achieved at room temperature. As temperature decreases, the currents through the Pt/BTO/SRO FTJs decrease by over about two orders of magnitude from 290 to 50 K. The indirect tunneling conduction, resulting from the phonon-assisted electron hopping through defect chains in the BTO barrier, is found to be responsible for the significantly temperature-dependent I-V characteristics of Pt/BTO/SRO. Direct tunneling conduction is observed below 50 K when defect-mediated tunneling currents are substantially suppressed. The ON/OFF ratio increases correspondingly by a factor of 3 with decreasing temperature. These results suggest that the reduction of defect density and then the suppression of indirect tunneling can greatly enhance the performance of FTJs and thus is a prerequisite for their future applications in non-destructive readout nonvolatile resistive ferroelectric memories.

This work was jointly sponsored by State Key Program for Basic Research of China (2009CB929503), Natural Science Foundation of China (Grant Nos. 91022001, 51222206, 11374139, and 51302139), and Natural Science Foundation of Jiangsu Province (BK2012016). The authors

are indebted to Dr. Scott A. Chambers from Pacific Northwest National Laboratory, the US, for polishing the language.

- <sup>1</sup>D. D. Fong, G. B. Stephenson, S. K. Streiffer, J. A. Eastman, O. Auciello, P. H. Fuoss, and C. Thompson, *Science* **304**, 1650 (2004).
- <sup>2</sup>E. Y. Tsymbal and H. Kohlstedt, *Science* **313**, 181 (2006).
- <sup>3</sup>E. Y. Tsymbal, A. Gruverman, V. Garcia, M. Bibes, and A. Barthélémy, *MRS Bull.* **37**, 138 (2012).
- <sup>4</sup>M. Ye, Zhuravlev, R. F. Sabirianov, S. S. Jaswal, and E. Y. Tsymbal, *Phys. Rev. Lett.* **94**, 246802 (2005).
- <sup>5</sup>V. Garcia, S. Fusil, K. Bouzehouane, S. Enouz-Vedrenne, N. D. Mathur, A. Barthélémy, and M. Bibes, *Nature* **460**, 81 (2009).
- <sup>6</sup>A. Gruverman, D. Wu, H. Lu, Y. Wang, H. W. Jang, C. M. Folkman, M. Ye, Zhuravlev, D. Felker, M. Rzechowski, C. B. Eom, and E. Y. Tsymbal, *Nano Lett.* **9**, 3539 (2009).
- <sup>7</sup>A. Crassous, V. Garcia, K. Bouzehouane, S. Fusil, A. H. G. Vlooswijk, G. Rispens, B. Noheda, M. Bibes, and A. Barthélémy, *Appl. Phys. Lett.* **96**, 042901 (2010).
- <sup>8</sup>A. Chanthbouala, A. Crassous, V. Garcia, K. Bouzehouane, S. Fusil, X. Moya, J. Allibe, B. Dlubak, J. Grollier, S. Xavier, C. Deranlot, A. Moshar, R. Proksch, N. D. Mathur, M. Bibes, and A. Barthélémy, *Nat. Nanotechnol.* **7**, 101 (2012).
- <sup>9</sup>H. Yamada, V. Garcia, S. Fusil, S. Boyn, M. Marinova, A. Gloter, S. Xavier, J. Grollier, E. Jacquet, C. Carrétéro, C. Deranlot, M. Bibes, and A. Barthélémy, *ACS Nano* **7**, 5385 (2013).
- <sup>10</sup>D. Pantel, S. Goetze, D. Hesse, and M. Alexe, *Nature Mater.* **11**, 289 (2012).
- <sup>11</sup>D. Pantel, H. Lu, S. Goetze, P. Werner, D. J. Kim, A. Gruverman, D. Hesse, and M. Alexe, *Appl. Phys. Lett.* **100**, 232902 (2012).
- <sup>12</sup>Y. W. Yin, J. D. Burton, Y. M. Kim, A. Y. Borisevich, S. J. Pennycook, S. M. Yang, T. W. Noh, A. Gruverman, X. G. Li, E. Y. Tsymbal, and Q. Li, *Nature Mater.* **12**, 397 (2013).
- <sup>13</sup>Z. Wen, C. Li, D. Wu, A. Li, and N. Ming, *Nature Mater.* **12**, 617 (2013).
- <sup>14</sup>M. Dawber, K. M. Rabe, and J. F. Scott, *Rev. Mod. Phys.* **77**, 1083 (2005).
- <sup>15</sup>R. J. Stratton, *J. Phys. Chem. Solids* **23**, 1177 (1962).
- <sup>16</sup>J. G. Simmons, *J. Appl. Phys.* **35**, 2655 (1964).
- <sup>17</sup>Y. Li and S. X. Wang, *J. Appl. Phys.* **91**, 7950 (2002).
- <sup>18</sup>B. Oliver and J. Nowak, *J. Appl. Phys.* **95**, 546 (2004).
- <sup>19</sup>Y. Lu, M. Tran, H. Jaffrès, P. Seneor, C. Deranlot, F. Petroff, J. M. George, B. Lepiné, S. Ababou, and G. Jézéquel, *Phys. Rev. Lett.* **102**, 176801 (2009).
- <sup>20</sup>Y. Xu, A. Matsuda, and M. R. Beasley, *Phys. Rev. B* **42**, 1492 (1990).
- <sup>21</sup>C. Höfener, J. B. Philipp, J. Klein, L. Alff, A. Marx, B. Büchner, and R. Gross, *Europhys. Lett.* **50**, 681 (2000).
- <sup>22</sup>Y. Lu, *J. Appl. Phys.* **102**, 123906 (2007).
- <sup>23</sup>L. I. Glazman and K. A. Matveev, *Sov. Phys. JETP* **67**(6), 1276 (1988), available at [http://www.jetp.ac.ru/cgi-bin/dn/e\\_067\\_06\\_1276.pdf](http://www.jetp.ac.ru/cgi-bin/dn/e_067_06_1276.pdf).